Available online at www.sciencedirect.com
ScienceDirect
Nuclear Instruments and Methods in Physics Research A 579 (2007) 812–816
NUCLEAR INSTRUMENTS & METHODS IN PHYSICS RESEARCH Section A
www.elsevier.com/locate/nima

Anomolous IV behavior of ATLAS SCT microstrip sensors

Y. Nakamura[a], K. Hara[a,*], K. Nakamura[a], K. Inoue[a], S. Shinma[a], Y. Ikegami[b], T. Kohriki[b], S. Terada[b], Y. Unno[b]

[a]*Institute of Pure and Applied Sciences, University of Tsukuba, 1-1-1 Tennodai, Tsukuba, Ibaraki 305-8571, Japan*
[b]*High Energy Accelerator Research Organization (KEK), Oho 1-1, Tsukuba, Ibaraki 305-0801, Japan*

Available online 31 May 2007

Abstract

We observe deteriorated IV, leakage-to-voltage, characteristics when the ATLAS SemiConductor Tracker (SCT) silicon microstrip detector is biased at a fixed voltage Vk for a long period. The leakage current is nearly halved at voltages below Vk. The noise figure is deteriorated and signal charge spreads to neighboring strips. The detector performance is, however, not degraded when biased at or above Vk. We characterize the observed phenomena in detail in this article.

PACS: 29.40

Keywords: Silicon; Microstrip; ATLAS; SCT; IV; Instability; Oxide layer; Hole trap

1. Introduction

Large-scale silicon microstrip detectors are instrumented in various particle physics experiments for their excellent spatial resolution, fast response and resistivity against radiation. At the LHC, for example, the ATLAS SemiConductor Tracker (SCT) [1] covers the region outside the PIXEL detector to perform precision tracking inside a 2 T magnetic field together with the straw-type proportional tubes of the Transition Radiation Tracker, located just outside of the SCT. The SCT consists of four concentric barrel layers composed of 2112 modules, and nine layers in each endcap composed of 1976 modules.

The barrel detector modules have been constructed at four qualified sites, including our Japanese site, where intensive, standardized quality assurance measurements were performed. In the course of our tests we eventually detected a noticeable increase in the noise figure as evaluated with test pulses implemented in the readout ASIC chips.

Our investigation was then extended to identify and understand this phenomenon, reaching the ultimate conclusion that detector performance is deteriorated when the bias voltage is lowered after having been maintained at a high value for an extended period. The deterioration is essentially manifested as a distortion of the IV curve accompanied by an observed degradation of interstrip isolation. The detector recovers by itself at the new, lower, bias voltage, but the recovery takes days or even weeks at low temperatures.

We describe the properties of the deteriorated IV curves of ATLAS SCT modules in Section 2. The impact on detector performance is given in Section 3 in terms of electrical noise and charge collection as evaluated by means of a Nd:YAG laser. The characteristics of this phenomenon, namely the magnitudes of deterioration and the recovery times, are evaluated at different temperatures as presented in Section 4.

2. Observation of deteriorated IV curves

All of the ATLAS SCT barrel sensors were fabricated by Hamamatsu Photonics (HPK) using 4″ wafer technology. There are 768 readout strips per sensor at a pitch of 80 μm. The p^+ implant electrodes are 16 μm wide and 63 mm long and biased through 1.5 MΩ poly-silicon resistors. The readout Al electrodes are 22 μm wide and are AC coupled

*Corresponding author.
E-mail address: hara@hep.px.tsukuba.ac.jp (K. Hara).

0168-9002/$ - see front matter © 2007 Elsevier B.V. All rights reserved.
doi:10.1016/j.nima.2007.05.300

to the implant strips via SiO_2 and Si_3N_4 layers. Four identical silicon microstrip sensors are paired, then glued back-to-back, maintaining a stereo angle of 40 mrad in the construction of an individual detector module.

Fig. 1 shows the IV curves measured every 4 h while the bias was kept at Vk = 350 V whenever the voltage was not ramped to obtain an IV curve. All IV scans went up to a maximum voltage of 500 V, unless otherwise noted. The temperature was 40 °C. The general feature that is observed after the bias voltage is lowered below Vk is that the leakage current is higher than expected in initial scans, and then decreases, asymptotically approaching an IV curve which has two plateaus, one below Vk and another above Vk. The latter is not determined by the full depletion voltage of the sensors which are typically around 80 V but rather by the long-term bias voltage Vk itself. Similarly deteriorated IV curves were observed for other modules, independent of whether they were operated in air or nitrogen.

Since the time when these sensors were prototyped, we have noticed that they initially exhibit a monotonically increasing IV curve that returns to the expected IV shape showing a clear shoulder corresponding to the full depletion voltage after a number of scans. This behavior is displayed in Fig. 1 as a sequence of curves between the scans labeled "1" and "2". A similar observation is reported in Ref. [2] for HPK large area strip sensors for IV curves measured with a ramping rate of 10 V/s while a normal IV curve is attained when the ramping rate is slowed to 1 V/min.

The transitional scans following scan "2" in Fig. 1, however, do not have a shape that can be explained by micro-discharge or conventional surface-charge effects. In addition, the transition takes much longer at lower temperatures, as described in detail in Section 4, which explains why the deterioration had escaped detection at 15 °C where we performed a 24 h stability test as a part of the SCT module quality assurance program.

The dependence of the second plateau on Vk is evident in Fig. 2, where Vk was chosen to be 150 V. This is a realistic operating voltage of the SCT modules at the beginning of the experiment. The IV curves are deteriorated in the voltage region below 140 V. This means that the detector will be operated in the deteriorated IV region if the bias voltage is lowered by more than 10 V after a substantial period of operation.

Fig. 3 shows the IV transition after Vk was lowered to 150 V after the sample had been biased at 350 V. Initially a deteriorated IV curve similar to the asymptotic curve shown in Fig. 1, labeled "12" is seen. The second plateau

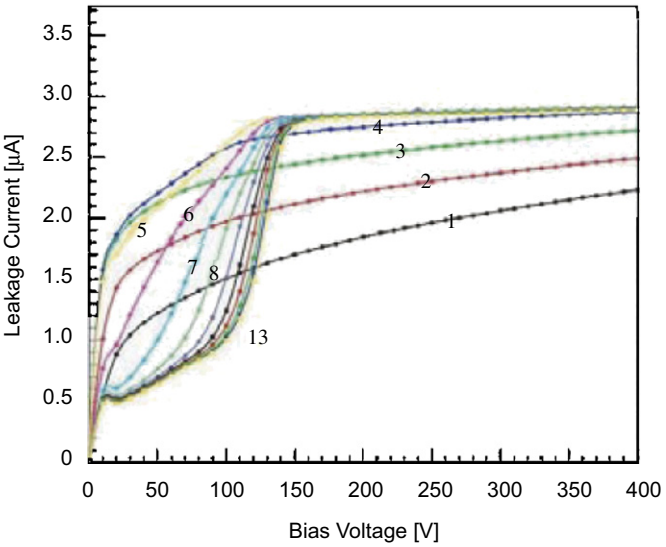

Fig. 2. IV curves of an SCT module measured every 4 h for Vk = 150 V. The sequence is as indicated by the numbers attached to the curves. The temperature is 40 °C.

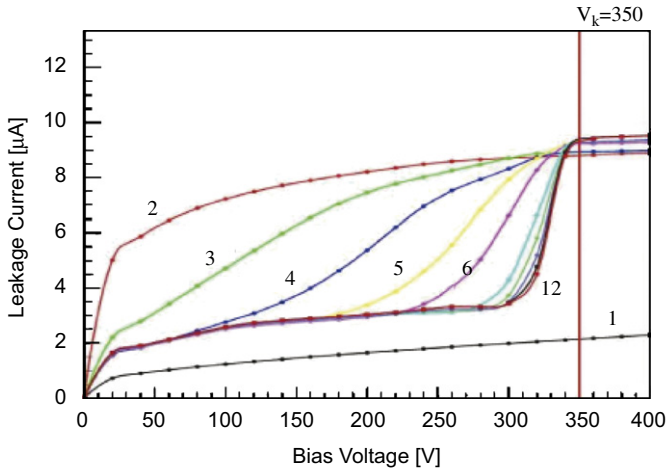

Fig. 1. IV curves of an SCT module measured every 4 h. The sequence is indicated by the numbers attached to the curves. The temperature is 40 °C. Vk, bias kept between the IV measurement, is 350 V.

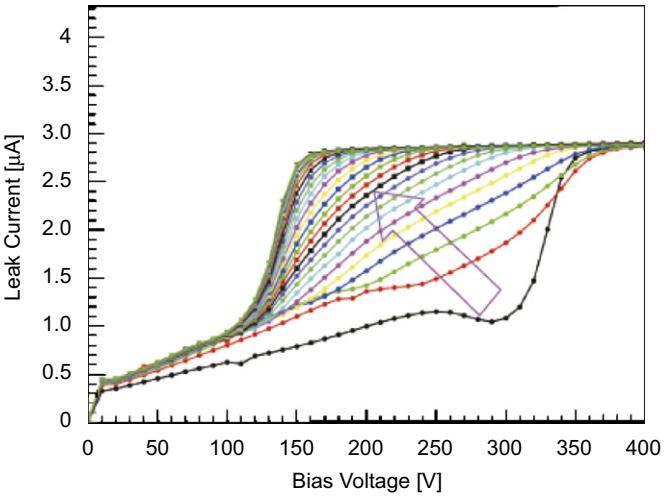

Fig. 3. IV curves of the same module of Fig. 1, measured every 2 h at temperature of 40 °C. Time zero is the time when Vk was lowered from 350 to 150 V after the IV curve had been stabilized at Vk = 350 V. The curves changed in the sequence indicated by the open arrow.

voltage decreased gradually from 340 to 140 V in about 40 h at 40 °C. Note that the asymptotic IV curve at 150 V is deteriorated in a manner similar to asymptotic curve "13" in Fig. 2, without showing a shoulder at the full depletion voltage.

The maximum voltage of 500 V in the IV scan was lowered for some samples, but the general observation remained the same. This excludes the possibility that 500 V might be too high for stable operation.

3. Detector performance under deteriorated conditions

As described above, we first noticed the degradation as an increase in the noise figure. In a module, a total of 1536, 12 cm long, strips are wirebonded to 12 ABCD3T chips [3]. The ABCD3T chip is a binary readout ASIC, composed mainly of amplifier-shaper and discriminator stages, followed by digital pipeline and output buffer stages. The DACs implemented in the chip perform the gain calibration by scanning the discriminator levels against variable input test charges. The noise figure, or equivalent input noise charge, is calculated at 1 fC input charge from the spread of the discrimination curve normalized by the chip gain.

The required noise figure is less than 1500 ENC so that a 1 fC threshold can be applied with negligible noise contributions, at a level of 5×10^{-4} or less. The average and rms spread of 1536 readout channels are listed in Table 1. The values at 150 and 350 V biases are given for the module operated at Vk = 350 V and at 40 °C. At 350 V, initial measurements exhibited noise slightly larger than the afore-mentioned requirement, but it soon decreased to a level of 1400 ENC. Since the noise level decreases with decreasing temperature at a rate of 5 ENC/° [3], both results are acceptable at about −10 °C where modules will be operated. The value at 150 V, however, increased with time, reaching a level of 1750 ENC. The increase seems to be correlated with the magnitude of deterioration seen in the IV curves (see Fig. 1).

The charge collection was evaluated by injecting light from a collimated Nd:YAG laser. This Q-switched, 1064 nm wavelength laser can simulate passage of charged particles. The details of the apparatus are described in Ref. [4]. The laser was collimated to 2×2 μm and injected right next to strip number 381 in the region between 381 and 382, one of the strips at the module center. The collected charge was measured together with that of neighboring strips. The result is shown in Fig. 4. Before the deterioration, the charge is collected essentially by strip 381 alone, with negligible charge sharing with neighboring strips. After the IV curve reached the asymptotic shape with Vk = 350 V, the charge collection is degraded in the voltage region below 300 V, showing a substantial charge sharing with strip number 382. The charge sum of strips 380–382, however, is comparable to that measured at time zero. This shows that the detector is fully depleted in the deteriorated voltage region. We also notice that the cross-talk to strip number 380 is not enhanced. This implies that the cross-talk is not through capacitive coupling but rather, the electric field is somehow disturbed so that some fraction of charge is directed to strip 382.

Similar deterioration was observed also when the laser was spotted at strips near the sensor edge, indicating the effect is probably present in the entire detector region.

Table 1
Average and one rms spread of the noise figures at 150 and 350 V, measured at different times after biasing at Vk = 350 V

	150 V		350 V	
	Average	rms	Average	rms
$T = 0$ ("1")	1452	72	1524	77
$T = 12$ h ("4")	1658	93	1395	72
$T = 40$ h (asympt)	1753	84	1397	67

The numbers "1" and "4" correspond to those in Fig. 1 and "asympt" is when the IV curve is stabilized.

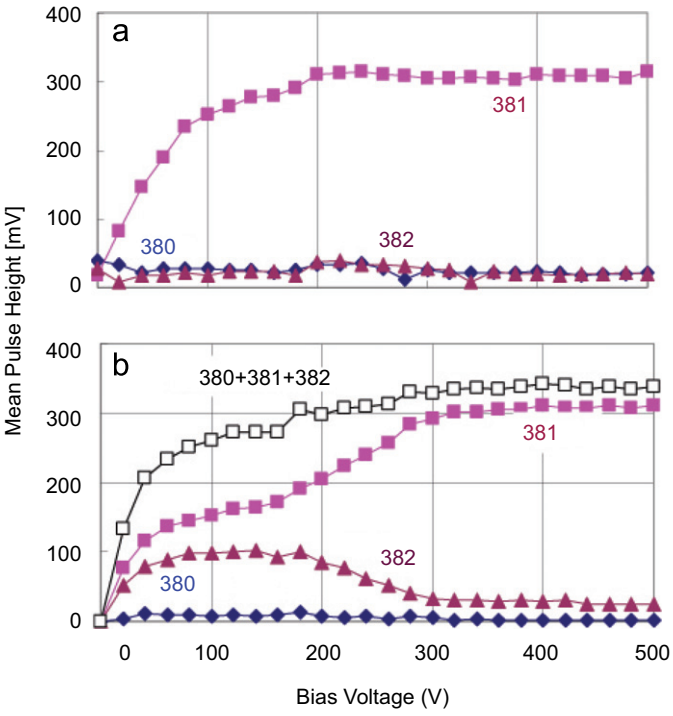

Fig. 4. Charge collection as a function of bias voltage for the same SCT module; (a) before, and (b) after the IV curve is deteriorated. The laser was spotted between strips 381 and 382 but close to strip 381. The collected charge is shown separately for strips 380–382 with the sum for (b).

4. Characteristics of IV deterioration

The study described in the previous section leads to a conclusion that noticeable performance degradation is inherently associated with the deterioration of the IV curve, but the performance should not be affected in the bias region at and above Vk. There is a margin of about 50 V judging from the charge collection curves. From the

point of view of detector operation, the detector should perform as expected as long as the bias is not lowered. Should the bias be lowered after a long time of operation, one must wait for the detector to recover from the deterioration.

The magnitudes of deterioration and the time constants for recovery were investigated with a single sensor. The difference with regard to a module is that the aluminum strip voltage is floating in the case of the single sensor. The evolution of IV curves measured for the single sensor is shown in Fig. 5, where the measurements for other sensor types, CDF Run2B [5] and CDF SVX L00 [6], are shown for comparison. The relevant parameters for the various sensor types are summarized in Table 2. All the sensors are p^+-on-n microstrips fabricated by HPK. The deterioration of IV curves is visible in the other sensor types, but the magnitudes and the voltage margins between the second plateau voltage and Vk are different. There is an observed tendency for the magnitude to be larger and the voltage margin to be smaller as the strip pitch is increased.

For quantitative discussion, we extracted characteristic parameters from the measured IV curves. In Fig. 6 we plot the leakage currents at a given voltage V_t (320 V in this case) against time. The current values are normalized by the value above Vk (350 V in this case). The transition can be fitted to a functional form to derive the asymptotic decrease A_r in magnitude of the normalized current, the time T_0 for the normalized current to decrease by $A_r/2$, and the one sigma spread T_s of the transition time. The fit results are given in the plot as an example. Among these, A_r and T_s can be extracted reliably, with about 10% uncertainty evaluated from repeated measurements, while T_0 depends on the voltage V_t and the initial conditions (namely; whether the detector was previously biased or not due to the effect described earlier for the difference of "1" and "2" in Fig. 1). Roughly speaking, T_0 is 3–5 times T_s, and the current reaches the asymptotic value in a time scale of 5–7 times T_s.

Using the data shown in Fig. 5, the fit indicated that the largest decrease in A_r, which occurs near Vk, is 14% for SVX2B and negligible for L00 sensors. Two SCT modules with ⟨1 1 1⟩ and ⟨1 0 0⟩ crystal orientations showed decreases of 51% and 61%, respectively. One SCT sensor with ⟨1 0 0⟩ showed a decrease of 58%. The magnitudes of deterioration are comparable for SCT modules and sensors, at a level that is about four times larger than that for SVX2B sensors. Since the ratio of the strip pitches is roughly 2, the magnitude is about twice the ratio of strip

Table 2
Main parameters of tested microstrip sensors

	ATLAS SCT	CDF Run2B	CDF L00
Strip pitch (μm)	80	37.5	25
Readout pitch (μm)	80	75	50
Implant width (μm)	16	8	5
Al width (μm)	22	14	7
Area (cm × cm)	6.4 × 6.4	3.9 × 9.4	0.8 × 8.6
HPK process	4″ or 6″	6″	4″
Wafer orientation	⟨1 1 1⟩ and ⟨1 0 0⟩	⟨1 0 0⟩	⟨1 1 1⟩

Run2B and L00 sensors are implemented with intermediate strip.

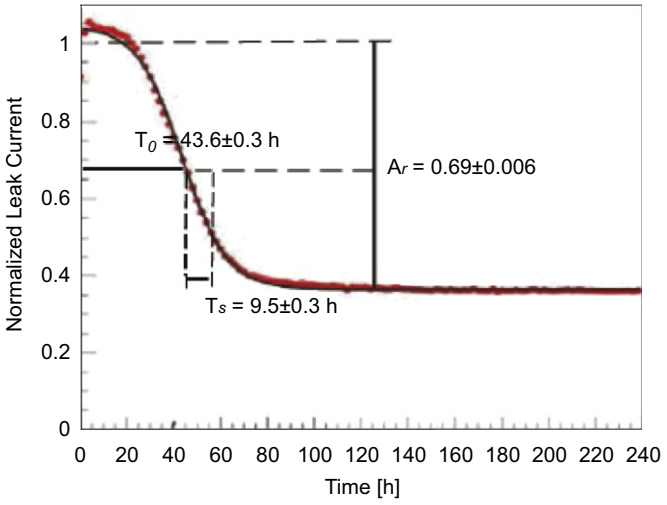

Fig. 6. The leakage currents at 320 V are plotted as a function of time for Vk = 250 V.

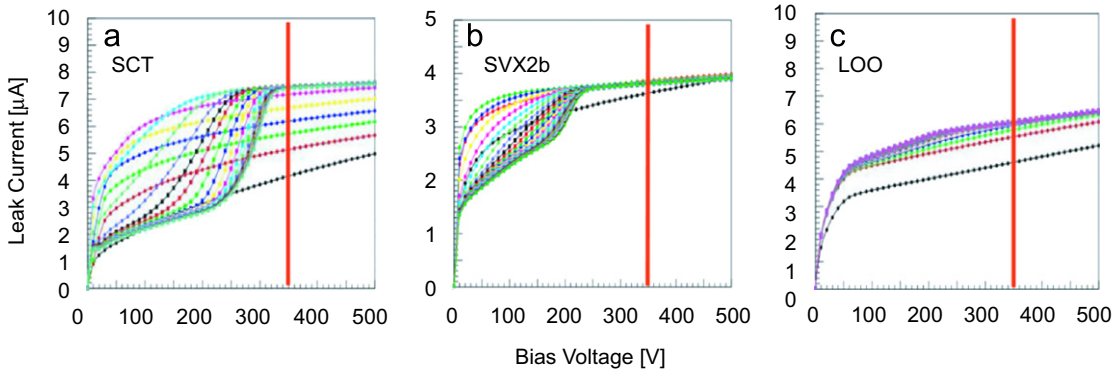

Fig. 5. IV curve transitions compared among (a) SCT, (b) CDF SVX2B, and (c) CDF SVX L00 sensors. The measurements were every 2 h at 40 °C with Vk = 350 V indicated by vertical lines. Transition sequences are similar for (a) and (b), gradual increases followed by decreases in lower bias voltage region. Though the magnitude of the decrease is tiny for (c), the general sequence agrees with (a) and (b).

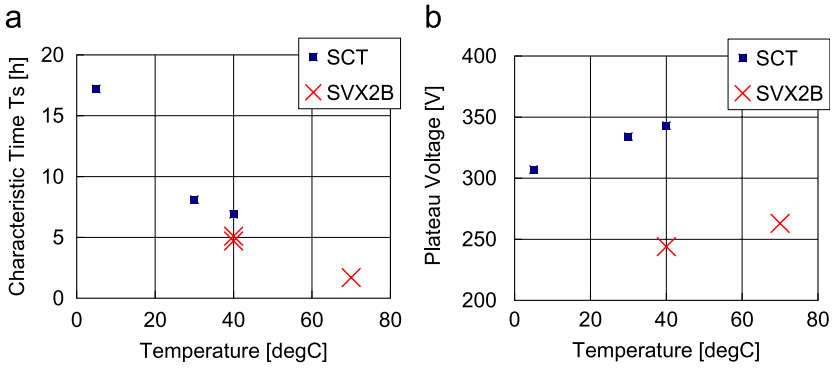

Fig. 7. (a) Characteristic time spread of deterioration transition and (b) the voltage where the second plateau is reached, as a function of the temperature.

pitches. There is a slight tendency seen for the sensors with ⟨1 0 0⟩ to be influenced more than those with ⟨1 1 1⟩.

Fig. 7a shows T_s measured at different temperatures from 5 to 70 °C. The temperature dependence can be well fitted to an exponential, resulting with

$$T_s = A\exp(-\alpha T) \quad \text{with } A \approx 20\,\text{h} \quad \text{and } \alpha = 0.030 - 0.032$$

where T is the temperature in centigrade. The total time to reach the asymptotic shape requires 5–7 times this value: 4–6 days at 0 °C and 6–8 days at −10 °C. The recovery times should be similar to theses time scales.

The voltage where the second plateau is reached is plotted in Fig. 7b as a function of temperature. The voltage decreases at lower temperature, providing a wider voltage margin for stable operation. The magnitude of deterioration A_r is found to exhibit only a weak dependence on the temperature.

5. Interpretation of the deterioration mechanism

The large, and temperature-dependent, characteristic recovery time constant may be related to slow movement of holes trapped in the oxide layer. The field strength around the strip was evaluated using a TCAD program [7]. Owing to the Al overhang relative to the implant strip, the maximum field locates inside the oxide layer. The maximum is calculated to be 1.3×10^6 V/cm for 350 V bias. The actual measured value will be different due to inaccurate modeling of detector processing, and also due to accumulation of charges that act to moderate the field strength. Holes traveling to the p^+ implant are slowed in the oxide. As the detector is kept biased, such holes together with electrons attracted to them should act to weaken the field, reaching an equilibrium. Once the bias is lowered (the field is reduced to 0.9×10^6 V/cm at 150 V), the trapped hole density is reduced in accord with the new bias level. The characteristic recovery time represents the time to rearrange the hole density.

Some efforts have been made to quickly recover from the deterioration, including UV illumination on the surface and forward-biasing for short times. Both turned out not to be effective, as would be expected if the problem is due to slow migration of holes.

6. Summary

We have observed unexpected IV characteristics when lowering the detector bias after having kept the bias constant for long periods. In the deteriorated IV region, the charge collection and noise figure are degraded. The deterioration recovers by itself, but requires days, and is especially slow at low temperature.

The detector performance is not degraded at and above the voltage where the detector has been biased. The characteristics described here must be taken into account when the detector bias is lowered.

References

[1] T. Kondo, et al., Nucl. Instr. and Meth. A 485 (2002) 47;
Y. Kato, et al., Nucl. Instr. and Meth. A 511 (2003) 132;
A. Abdesselam, et al., Nucl. Instr. and Meth. A 568 (2006) 642.
[2] S. Yoshida, et al., IEEE Trans. Nucl. Sci. NS 49 (2002) 1017.
[3] F. Campabadal, et al., Nucl. Instr. and Meth. A 552 (2005) 292.
[4] K. Hara, et al., Nucl. Instr. and Meth. A 541 (2005) 122.
[5] T. Akimoto, et al., IEEE Trans. Nucl. Sci. NS 51 (2004) 1546.
[6] T.K. Nelson, for the CDF II Collaboration, The CDF Layer 00 Detector, Int. J. Mod. Phys. A 16S1C (2001) 1091.
[7] SILVACO International, 4701 Patrick Henry Drive, Santa Clara, CA.